Acta Crystallographica Section A
Foundations of Crystallography
ISSN 0108-7673

Received 28 January 2000
Accepted 13 July 2000

A model for diffraction from MCM-41 materials

Z. Tun* and P. C. Mason

National Research Council of Canada, Neutron Program for Materials Research, Chalk River, Ontario, Canada K0J 1J0. Correspondence e-mail: zin.tun@nrc.ca

A model involving only a small number of parameters provides a convenient way of interpreting diffraction patterns from MCM-41 materials. Each parameter of the model has a clear physical meaning, and this approach is clearly superior to extracting pore structure information by fitting Gaussians to an observed diffraction pattern.

1. Introduction

The class of porous materials known by the designation MCM-41 has attracted much attention since their synthesis was first reported by Kresge *et al.* (1992). Unlike many other porous materials, the pores of MCM-41 are long cylinders of uniform diameter, packed uniaxially to form a quasi-periodic hexagonal lattice. Moreover, the pore diameter is adjustable over an approximate range of 1 to 10 nm by varying the size of template materials used to form the pores. With the relative volume of the pores constituting a very large volume fraction (up to 80%) of a typical sample, MCM-41 materials are well suited for studies ranging from capillary melting (Edler *et al.*, 1996), adsorption/desorption of gases (Rathousky *et al.*, 1995) and studies of molecules in confined geometries (Baker *et al.*, 1997; Takahara *et al.*, 1999). The chemistry of MCM-41 materials, the pore formation mechanism and the numerous applications these materials offer have been recently reviewed by Ying *et al.* (1999).

In general, the synthesis begins with mixing a silicate solution with a surfactant that self-assembles into cylindrical micelles. The cylinders are straight over long distances and the length greatly exceeds the diameter. The length of the hydrocarbon tails of the surfactant determines the cylinder diameter. At a sufficiently high density, these cylindrical micelles pack into a hexagonal arrangement with the silicate particles occupying the areas around the head groups of the surfactant and the packing voids between cylinders. With this structure formed, the surfactant is removed by heat processing, leaving the silicate as a porous matrix. The resultant pores are nearly the same size and shape as the template micelles.

Diffraction studies of MCM-41 have confirmed the hexagonal arrangement of the pores (Kresge *et al.*, 1992). However, the observed diffraction peaks are intrinsically wide and fall off rapidly in intensity, indicating that there is a degree of disorder present within the system. One of the best X-ray results of which we are aware, for instance, goes only to third order (Edler *et al.*, 1997). As a tool for analysing such a diffraction pattern, we here propose a model that includes a conceptually simple disorder (§2), followed by the calculation of the expected diffraction pattern (§3). Finally, we will explore how the calculated pattern changes as a function of model parameters (§4).

2. Description of the model

The model is an array of infinitely long cylinders of finite radius r (*e.g.* 15 Å) arranged in a hexagonal array within a host material. The arrangement, however, is not perfect. If we define a *perfect* hexagonal lattice by choosing one of the cylinders as the origin, the nearest-neighbour cylinders more or less lie on lattice points but the order is progressively lost for cylinders further from the origin. The lattice parameter of the perfect lattice is a (*e.g.* 40 Å) and, since there is always some host material between adjacent cylinders, a is necessarily $>2r$. We define a displacement vector $\mathbf{u}_l$ which is the measure of displacement of a cylinder from its ideal lattice position $\mathbf{l}$. Since the 'errors' caused by non-perfect arrangement accumulate at larger distances, the magnitude of $\mathbf{u}_l$, on average, increases with the length of $\mathbf{l}$. In order to achieve simple analytical results, we propose that the distribution of $\mathbf{u}_l$ with a value of $|\mathbf{l}|$ is a Gaussian whose variance is given by

$$\langle u_l^2 \rangle = \varepsilon |\mathbf{l}|. \qquad (1)$$

The constant ε is an important model parameter as it controls how quickly the order is lost as one moves away from the arbitrarily chosen origin. The dimensions of ε, a, r, u and l are all ångstroms. In addition, one can define an overall size, $R_{\rm limit}$, of the array over which (1) is valid. This size could range from ~100 Å (small array), to a few thousand ångstroms (large array), to infinity (micrometre-size array). Note that $R_{\rm limit}$ is not necessarily the physical size of a sample or the size of individual grains in the case of a powder sample. Rather, it is the typical size of a 'correlated region'.

The model we propose above is not conceptually new. It is a special case of the hexagonal paracrystalline lattice described by Hosemann & Bagchi (1962) where the degree of order is relatively high. In the vocabulary of these authors, the order in

MCM-41 is high enough to produce 'discontinuous small-angle scattering', *i.e.* more than one interference maximum exists in the calculated structure factor.

We now consider the contrast that can be detected with a diffraction experiment. If the experiment is limited to small scattering angles so as not to see diffraction corresponding to the atomic spacings, we are sensitive only to the 'density' difference between the host material and the cylinders. Let ρ be the difference and, for simplicity, we arbitrarily assign the host material a density of zero and that of the cylinders ρ. For X-ray diffraction, ρ is given by electron density times the classical radius of an electron, and for neutron diffraction it is the difference in scattering-length densities of the materials concerned.

3. $S(\mathbf{Q})$ of the model

We will carry out the calculation in two parts: (i) the form factor of an individual pore represented by a cylinder, and (ii) the lattice sum over the points that are arranged in the imperfect hexagonal array. The two parts are subsequently combined by means of the convolution theorem to calculate the overall scattering cross section $S(\mathbf{Q})$.

3.1. Form factor of a cylinder

The form factor of a cylinder that is infinitely long in the z direction and has a radius r is given by the Fourier transform

$$F_c(\mathbf{Q}) = \int \rho(\mathbf{r}) \exp(i\mathbf{Q}\cdot\mathbf{r})\, \mathrm{d}\mathbf{r}, \tag{2}$$

where

$$\rho(\mathbf{r}) = \begin{cases} \rho & \text{if the } xy \text{ projection of } \mathbf{r},\ r_{xy} \leq r \\ 0 & \text{if } r_{xy} > r. \end{cases}$$

The result is the Fourier transform of a circle, given in terms of the Bessel function $J_1(rQ_{xy})$, times a δ function in the z direction.

$$F_c(\mathbf{Q}) = (2\pi r\rho/Q_{xy}) J_1(rQ_{xy})\delta(Q_z). \tag{3}$$

The δ function indicates that one can only see diffraction from an infinite cylinder if its axis is perpendicular to $\mathbf{Q}$. This has an important effect for powder specimens where each grain contains parallel pores but the grain orientation is random. If one collects diffraction data using a standard diffractometer (monochromatic incident beam and a single detector that scans in the horizontal plane), the measured intensity at a particular $\mathbf{Q}$ comes only from those grains that are so oriented that their pores are perpendicular to $\mathbf{Q}$. If ΔQ_z is the vertical size of the resolution 'window' of the diffractometer, the number of gains contributing to measured intensity is directly proportional to the ratio $(\Delta Q_z/Q)$, a factor that needs to be included in analysing the data.

For a long but finite-length cylinder, the δ function broadens into a Gaussian peak. Provided the width of the Gaussian is much less than ΔQ_z, the above discussion on the effect of vertical resolution is valid.

3.2. Lattice sum over points arranged in an imperfect hexagonal array

We now consider the imperfect hexagonal array as explained in §2. However, instead of cylinders, we consider a 2D array of scattering centres that mark the geometrical centres of the cylinders. The scattering cross section of any collection of scattering centres, in the limit of weak scattering, is given by

$$S_o(\mathbf{Q}) = F_o^*(\mathbf{Q}) F_o(\mathbf{Q}), \tag{4}$$

where

$$F_o(\mathbf{Q}) = \sum_j \exp(i\mathbf{Q}\cdot\mathbf{R}_j) \tag{5}$$

is the geometrical structure factor. The index j is defined such that $\mathbf{R}_j$ is a vector terminating at scattering centre j.

For a small array, we can evaluate the sum of (5) numerically. For large and infinite arrays, we will evaluate the sum statistically by arguing that the scattering centres are all equivalent and their surroundings, on average, are identical. The lattice vector $\mathbf{l}$ is the position of $\mathbf{R}_j$ if we had a perfect hexagonal lattice, *i.e.*

$$\mathbf{R}_j = \mathbf{l} + \mathbf{u}_l.$$

Therefore,

$$F_o(\mathbf{Q}) = \sum_l \exp(i\mathbf{Q}\cdot\mathbf{l}) \langle \exp(i\mathbf{Q}\cdot\mathbf{u}_l)\rangle. \tag{6}$$

The symbol $\langle \ldots \rangle$ indicates that we will have to evaluate this exponential for a typical distribution of $\mathbf{u}_l$. In terms of $\mathbf{u}_l$, the projection of $\mathbf{u}_l$ onto $\mathbf{Q}$ and a Gaussian distribution $g(u_l')$, we evaluate

$$\int_{-\infty}^{\infty} \exp(iQu_l') g(u_l')\, \mathrm{d}u_l' = \exp(-\tfrac{1}{4}Q^2\varepsilon|l|). \tag{7}$$

In the last step, we have made used of the fact that the direction of $\mathbf{u}_l$ is random and

$$\langle u_l'^2\rangle = \tfrac{1}{2}\langle u_l^2\rangle$$

for any projection.

Substituting (7) in (6) gives

$$F_o(\mathbf{Q}) = \sum_l \exp(i\mathbf{Q}\cdot\mathbf{l}) \exp(-\tfrac{1}{4}Q^2\varepsilon|l|). \tag{8}$$

There are several (approximate) ways of evaluating the above 2D-lattice sum. The most obvious way, of course, is to do the sum numerically to a cut-off R_{limit}. However, a further insight of the 2D sum could be obtained by first considering the result of a 1D sum along a certain direction in real space. We present the following case study as an example.

3.3. The 1D sum along the *a* axis

As a subset of the terms contained in (8), let us evaluate the sum

$$F_o^{1D}(\mathbf{Q}) = \sum_n \exp(i\mathbf{Q}\cdot\mathbf{a}n) \exp(-\tfrac{1}{4}Q^2\varepsilon a|n|), \tag{9}$$

where n is an integer. This sum is easily carried out as two geometric progression series, giving

$$F_o^{1D}(\mathbf{Q}) = \frac{\sinh(\frac{1}{4}Q^2\varepsilon a)}{\cosh(\frac{1}{4}Q^2\varepsilon a) - \cos(\mathbf{Q}\cdot\mathbf{a})}. \quad (10)$$

The 1D sum for $\mathbf{Q}||\mathbf{a}$, $a = 40$ Å and $\varepsilon = 0.4$ Å is plotted in Fig. 1. The variation of F_o^{1D} looks very much like scattering from a liquid, as first pointed out by Emery & Axe (1978) (also see Axe, 1980). The periodicity is due to the $\cos(\mathbf{Q}\cdot\mathbf{a})$ term in the denominator as the hyperbolic functions show only monotonic variations. Had we performed the 1D sum along another direction in real space, the only change in (10) would be that $\mathbf{a}$ is replaced by $\mathbf{d}$, a vector from the origin to the first lattice point encountered in the chosen direction. Consequently, the plot would look identical to Fig. 1 except that the Lorentzian-like peaks would appear at different positions. The 2D sum of (8) is a linear combination of these 1D sums, each weighted in proportion to the density of lattice points, which is simply $(1/d)$. Since the lattice-point density is highest along $\mathbf{a}$, F_o^{1D} along $\mathbf{a}$ is the leading order contribution to the 2D sum. We expect the result of the 2D sum to look similar to Fig. 1 except that $|F_o|$ between peaks is considerably increased by the contributions from other directions.

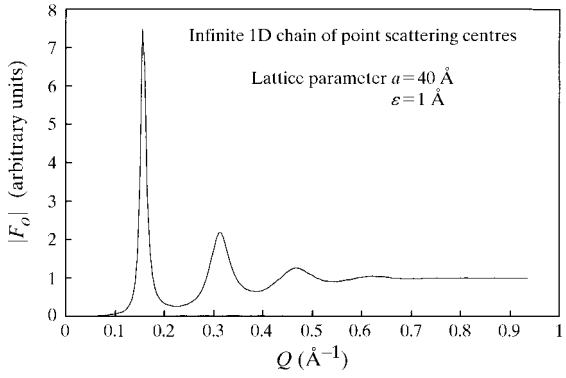

Figure 1
Geometrical structure factor of 1D array of point scattering centres. The array is infinitely long but the order between the centres is gradually lost with distance owing to the parameter ε as explained in the text.

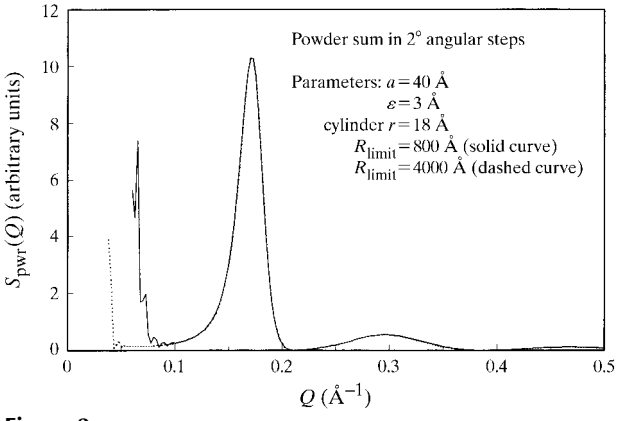

Figure 2
Powder-averaged $S(\mathbf{Q})$ of infinitely long cylinders, packed into an *imperfect* hexagonal array. The 2D lattice sum of the array was carried out numerically from the centre to a radius $R_{limit} = 800$ Å (solid curve) or to $R_{limit} = 4000$ Å (dashed curve). The two results differ appreciably only for $Q < 0.1$ Å^{-1}.

3.4. Numerical evaluation of the 2D sum and $S(\mathbf{Q})$ for powder samples

We now return to computing $S(\mathbf{Q})$. The results in (3) and (8) can be combined to give the structure factor of an imperfect hexagonal array of finite-radius cylinders whose magnitude squared is $S(\mathbf{Q})$.

$$S(\mathbf{Q}) = |F_o(\mathbf{Q})F_c(\mathbf{Q})|^2. \quad (11)$$

The above equation gives $S(\mathbf{Q})$ of a single correlated region, a result analogous to that of a single crystal. However, most diffraction studies on MCM-41 materials are performed with powder samples. Even if one manages to do diffraction from a single grain of sample (say using synchrotron radiation), it is likely that the parallel pores of the grain form many correlated regions, in which case one will still measure the 'powder averaged' $S(\mathbf{Q})$ but without the $1/Q$ vertical resolution correction factor [see (3)]. In the discussion below, we will denote this quantity as $S_{pwr}(\mathbf{Q})$.

4. Discussion

Fig. 2 shows $S_{pwr}(\mathbf{Q})$ for a model we believe to represent the majority of MCM-41 materials. For the solid curve, the 2D sum of (8) was carried out to $R_{limit} = 800$ Å, with the parameters $a = 40$ Å and $\varepsilon = 3$ Å. Note that the r.m.s. value $(R_{limit}\varepsilon)^{1/2} = 49$ Å is larger than a, *i.e.* the order is lost by the time the sum reaches the boundary of the correlated region. For powder averaging, the calculation was repeated for different directions of $\mathbf{Q}$ between [1,0] and [1,1] directions at every 2°. Tests showed that this angular step was sufficiently small for the width of the peaks.[1]

The resultant $S_{pwr}(\mathbf{Q})$ contains two well defined peaks. The one at $Q \approx 0.18$ Å^{-1} is the (1,0) peak, the lowest-order peak expected for the structure. The peak at $Q \approx 0.3$ Å^{-1} is actually the superposition of (1,1) and (2,0) peaks, both very much reduced in intensity and increased in width by the effects of parameter ε (the form factor is also responsible for reduced intensity). The solid curve shows extra scattering at Q values below 0.1 Å^{-1}, which is the onset of small-angle scattering caused by the finite size of R_{limit}. We can verify this by repeating the 2D sum over a much longer range with R_{limit} set to 4000 Å. The result, shown as the dashed curve, is indistinguishable from the solid curve except for the low-Q region.

It should be appreciated that ε is an essential parameter for successful modelling of scattering from MCM-41 materials. For instance, one cannot try to induce width in the diffraction peaks by simply reducing the size of the correlated regions. As a demonstration, we show in Fig. 3 the diffraction from a hypothetical model with $\varepsilon \rightarrow 0$ and R_{limit} greatly reduced (*i.e.*

[1] The 2° step may not be sufficiently small if one attempts to least-squares fit the model to a measured diffraction pattern. For that purpose, the angular step size should be either the incident-beam collimation used for data collection or the transverse width of the calculated peaks *before* powder averaging, whichever is larger.

perfect hexagonal arrangement over a short distance). The peaks that correspond to the 40 Å lattice parameter, or the primary peaks, do get wider, and the region between those peaks is filled with secondary maxima resulting from the very short $R_{\rm limit}$. Note that the acquired width of the primary peaks is order-independent, as shown by the FWHM values written in the figure. In contrast, the width arising from non-zero ε increases rapidly with Q (this effect is most apparent in Fig. 1).

The aim of many diffraction studies on MCM-41 is to see a change in the diffraction pattern when the pores of the structure are filled with a foreign material such as hydrocarbons or water. Altering the constituent of the pores does not affect $F_o(\mathbf{Q})$, but the diffraction pattern changes because of a change in the form factor $F_c(\mathbf{Q})$. When foreign materials are successfully incorporated into MCM-41, there are two scenarios: (I) the material fills the pores completely, or (II) the material coats the inside wall of the pores, leaving a vacant space in the middle. We will now use the proposed model to explore how sensitive diffraction techniques can be in differentiating these two scenarios.

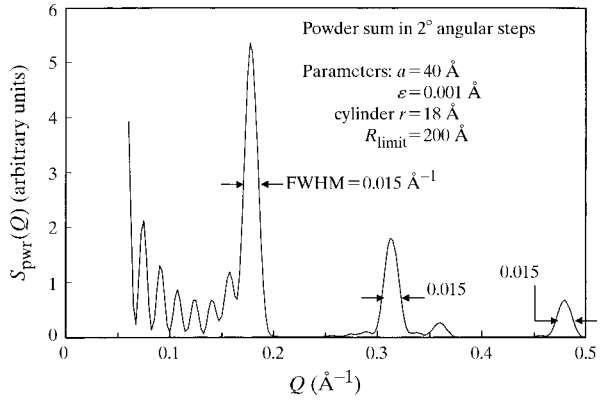

Figure 3
Powder-averaged $S(\mathbf{Q})$ of infinitely long cylinders packed into a *perfect* hexagonal array of very small size. The array extends only for ten (*i.e.* $2R_{\rm limit}/a$ = 10) lattice spacings.

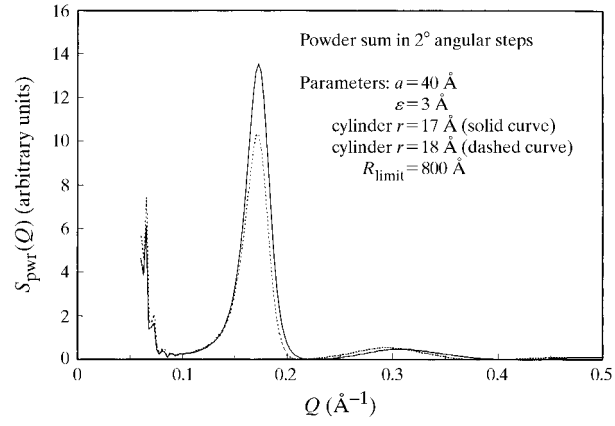

Figure 4
The effect on $S_{\rm pwr}(\mathbf{Q})$ when the radius of individual pores is changed from 18 Å (dashed curve) to 17 Å (solid curve). Such a change is expected for MCM-41 when the inside walls of the pores are coated with a thin layer of a material that is contrast matched to the host.

Scenario (I): In general, the foreign material will have a 'density' different from the host material and the original constituent of the pore (*e.g.* empty space). Therefore, filling the pores completely with a foreign material will change the contrast factor ρ in (3). The measured absolute intensities will change but the shape of the diffraction pattern remains the same. However, if one could 'contrast match' the foreign material to the host (often an easy task for neutron diffraction), the diffraction pattern will completely disappear.

Scenario (II): The form-factor calculation will be more complicated because each pore now is a cylinder of finite wall thickness, with the wall density different from that of both the host material and the central core. Again, if the foreign material is contrast matched to the host material, the analysis is simpler – the diffraction pattern would change as if the cylinder radius were smaller. We show in Fig. 4 how sensitive diffraction is to this change. The model represented by the solid curve is identical to Fig. 2 (replotted as the dashed curve) except that the form-factor radius is reduced by 1 Å. Note that not only the absolute but also the relative intensities of the peaks change – a change that is far easier to detect in an experiment.

5. Conclusions

The model we have presented is generally applicable in describing the scattering from MCM-41 materials. We show that variations in a relatively small parameter set can produce markedly different diffraction patterns. The model therefore allows for easy analysis and comparison of bare MCM-41 materials as well as the systems that use MCM-41 as a host matrix.

We expect that the basic concept, *i.e.* a local order that is lost gradually with distance, can be applied to a wide range of problems involving self-organized quasi-periodic structures. Indeed, it is an easy task to introduce different functional forms of 'disorder' in case the simple linear (and isotropic) disorder is found to be inadequate for a new class of materials.

References

Axe, J. D. (1980). *Ordering in Strongly Fluctuating Condensed Matter Systems*, edited by T. Riste, pp. 399–414. *NATO Advanced Study Institute, Geilo, Norway*. New York: Plenum.

Baker, J. M., Dore, J. C. & Behrens, P. (1997). *J. Phys. Chem.* B**101**, 6226–6229.

Edler, K. J., Reynolds, P. A., Trouw, F. & White, J. W. (1996). *Chem. Phys. Lett.* **249**, 438–443.

Edler, K. J., Reynolds, P. A., White, J. W. & Cookson, D. (1997). *J. Chem. Soc. Faraday Trans.* **93**, 199–202.

Emery, V. J. & Axe, J. D. (1978). *Phys. Rev. Lett.* **40**, 1507–1511.

Hosemann, R. & Bagchi, S. N. (1962). *Direct Analysis of Diffraction by Matter.* Amsterdam: North-Holland.

Kresge, C. T., Leonowicz, M. E., Roth, W. J., Vartuli, J. C. & Beck, J. S. (1992). *Nature (London)*, **359**, 710–712.

Rathousky, J., Zukal, A., Franke, O. & Schulz-Ekloff, G. (1995). *J. Chem. Soc. Faraday Trans.* **91**, 937–940.

Takahara, S., Nakano, M., Kittaka, S., Kuroda, Y., Mori, T., Hamano, H. & Yamaguchi, T. (1999). *J. Phys. Chem.* B**103**, 5814–5819.

Ying, J. Y., Mehnert, C. P. & Wong, M. S. (1999). *Angew. Chem. Int. Ed. Engl.* **38**, 56–77.